

A QXP-Based Multistep Docking Procedure for Accurate Prediction of Protein–Ligand Complexes

Laleh Alisaraie, Lars A. Haller, and Gregor Fels*

Department of Chemistry, University of Paderborn, Warburger Str. 100, D-33098 Paderborn, Germany

Received August 25, 2005

The two great challenges of the docking process are the prediction of ligand poses in a protein binding site and the scoring of the docked poses. Ligands that are composed of extended chains in their molecular structure display the most difficulties, predominantly because of the torsional flexibility. On the basis of the molecular docking program QXP-Flo+0802, we have developed a procedure particularly for ligands with a high degree of rotational freedom that allows the accurate prediction of the orientation and conformation of ligands in protein binding sites. Starting from an initial full Monte Carlo docking experiment, this was achieved by performing a series of successive multistep docking runs using a local Monte Carlo search with a restricted rotational angle, by which the conformational search space is limited. The method was established by using a highly flexible acetylcholinesterase inhibitor and has been applied to a number of challenging protein–ligand complexes known from the literature.

INTRODUCTION

Molecular docking programs play an essential role in the modern drug discovery process. They help to identify the correct binding mode of a ligand in its binding site of a protein and to yield an affinity-based rank order for a series of ligands bound to a particular binding pocket.^{1–5} Most docking algorithms are able to generate a large number of possible structures, and they also provide a means to score each structure, to identify the energetically favored binding mode. Search algorithms and scoring functions are, therefore, the fundamental parts of docking programs.

The docking process can be broken down into five phases, which are the modeling of the target, generating the possible conformations of the ligand, docking each conformation, scoring each docked ligand, and selecting candidate ligands for further investigations.⁶ High-resolution X-ray crystallographic protein structures are routinely used for ligand docking. In addition, structures derived from NMR experiments or those predicted by homology modeling may also be used. If the target protein is extracted from a structure in which a ligand is bound to the protein, the docking experiments using that structure are termed “bound docking” throughout this paper; otherwise, for simplicity, the experiments are termed “unbound docking”.⁷ It should be noted, however, that a truly unbound docking would require the target binding site to be in a free unbiased conformation, for example, the apo form of the protein.

Docking procedures as part of a drug development process usually involve unbound docking because it generates the pose prediction of a new ligand in the binding site of a known protein. On the other hand, because of the conformational changes that occur between the liganded and unliganded forms of proteins, performing bound docking usually yields better results.

Therefore, the components required for a docking experiment are a target protein with or without a bound ligand, the molecule of interest, and a computational framework that allows the implementation of the desired docking and scoring procedures.⁸ The crystal structure of a protein–liganded or unliganded—is still the most important source for a structure-based design of new or improved ligands by way of docking studies. High-resolution protein crystal structures are increasingly available because of the efforts of the human genome project and high-throughput crystallography techniques, resulting in a total of about 35 000 protein structures having been deposited in the Protein Data Bank as of February 2006.⁹

A comparison of a variety of docking programs has recently been published.¹⁰ In addition, a more general description of the advances in docking and scoring algorithms⁸ and a survey of the impact of docking, scoring, and scoring functions are given elsewhere.^{1,7,11–15} Different search algorithms have been developed which basically differ in the generation of ligand poses in the binding site. Programs such as FlexX,¹⁶ DOCK,¹⁷ and Hammerhead¹⁸ build up the ligand in the binding site starting from a base fragment, while QXP,¹⁹ AutoDock,²⁰ GOLD,²¹ and ICM-Dock²² treat the ligand in its entirety.

Structural investigations of acetylcholinesterase (AChE),^{23–25} a serin protease responsible for the termination of signal transmission at cholinergic synapses by cleavage of the neurotransmitter acetylcholine, have resulted in a detailed knowledge of the substrate binding site. On the basis of these data, we have successfully predicted the pose of the AChE inhibitor galanthamine in the active site, particularly employing AutoDock²⁶ and QXP²⁷ as docking tools. The active site of this enzyme is located at the lower end of a gorge that extends 20 Å down into the protein. In addition to the cleavage site at the bottom of the gorge, there is a peripheral anionic site at its upper end, believed to play an important role in the formation of β -amyloid plaques, which finally

*Corresponding author tel.: +49-5251-602181; e-mail: fels@uni-paderborn.de.

leads to selective neuronal loss in cholinergic population and the death of the particular synapse as a cause for Alzheimer's disease.²⁸ These biochemical processes have led to the idea of bis-functional ligands that can simultaneously block the catalytic triad and the anionic subsite at opposite sites of the gorge.^{29–31} Ligands that span the gorge will be of 15–20 Å length and, therefore, usually will contain a comparatively large number of rotatable single bonds. Compared to the flexibility of small molecules, the flexibility issue in ligands with extended structures is still a remaining problem of molecular docking. Depending on the docking tool employed, a bis-functional AChE inhibitor resulting from docking studies can show a varying spacer length, even though the two ends of the extended ligand structure still bind almost identically to the upper and lower ends of the AChE gorge.³¹

Because this finding certainly is not a special situation in the case of AChE ligands but rather will be true for any extended ligand structure binding to any protein, we were interested to find a docking procedure that is particularly suited for highly flexible ligands while, at the same time, maintains its applicability to smaller ligands with less conformational variation. The flexibility of a ligand increases dramatically with an increasing number of rotatable bonds, with a result of a vast growing number of conformers that all could potentially represent the active ligand conformation. Following our earlier results on galanthamine docking to AChE,²⁷ derived from the docking algorithm of QXP, we have developed a consensus molecular docking approach utilizing two different ranking procedures that can be deduced from the various output data of the QXP program. First, we make use of the scoring function of QXP, which directs the search strategy of the docking algorithm and ranks the resulting docking solutions according to their total estimated binding energy (E_{ass}). Besides that, and most importantly, we apply a second scoring procedure which separately takes into account the available energy terms for the 25 results of a conventional QXP run. In particular, from the QXP output, we have employed the total energy of nonbonded interactions (E_{nbd}), van der Waals energy (vdW), the positive van der Waals energy (vdW+), the electrostatic energy (E_{est}), the contact energy of interactions (E_{cnt}), and the number of hydrophobic contacts (N_{hph}). For details, see the Materials and Methods section. These data are independently used to yield a single, final score. As long as the best E_{ass} and the highest consensus score do not reside on the same structure, the docking procedure is repeated starting from the highest consensus score structure as input for the next run. This QXP-based multistep docking procedure (QXP-MSD) always utilizes full Monte Carlo (MC) conditions^{32,33} in the first run and a local-MC variation^{34,35} in all subsequent runs. The local-MC search algorithm (LMCS) reduces the degree of freedom of a molecule by random selection of the rotational angle in the interval of 20–30° rather than 360° as in the full-MC search. The procedure is terminated when a given docking result simultaneously shows the highest consensus score and the lowest total E_{ass} .

The method was developed using bound docking experiments of a highly flexible ligand, that is, employing a known crystal structure so that the correctness and the quality of the docking results could be deduced from root-mean-square deviation (RMSD) calculations. To this end, we have used

Table 1. Data Set of Ligands and Proteins Used

ligand	ID	protein	PDB code of complex	ref
galanthamine	1	acetylcholinesterase	1QTI	38
			1DX6	39
BHG	2	acetylcholinesterase	unpublished	37
E2020	3	acetylcholinesterase	1EVE	40
decamethonium	4	acetylcholinesterase	1ACL	41
WIN51711	5	poliovirus	1PIV	42
WIN52084	6	rhinovirus 14	1RUH	43
arachidonic acid	7	cyclooxygenase	1DIY	44
methylamino-phenylalanyl-leucylhydroxamate	8	human neutrophil collagenase	1MNC	45
deoxythymidine	9	thymidine kinase	1KIM	46
		thymidine kinase	1KI6	46
		thymidine kinase	1KI7	46
		thymidine kinase	1KI8	46
oxindole	10	cyclin-dependent kinase 2 (Cdk2)	1FVT	47

the AChE inhibitor benzosulfimidoethylgalanthamine (BHG, **2**), a galanthamine derivative that has a benzosulfimido group (saccharino group) linked to the galanthamine core by a hexamethylene spacer. The crystal structure of BHG (**2**), a compound synthesized in the laboratory of Jordis et al.,³⁶ has been solved by the group of Lamba³⁷ and was made available to us prior to publication. We have further evaluated the method by using a variety of other ligands, placing particular emphasis on flexible ligands that usually are the most difficult to reproduce by docking experiments (see Table 1). In addition, we have also performed unbound docking experiments to assess the success of the procedure in the more usual and frequent case of unbound docking, that is, for the prediction of unknown structures of protein–ligand complexes. In this respect, we have employed different inhibitors of AChE and other protein targets such as rhinovirus protein, cyclooxygenase, collagenase, and CDK2. The proteins and inhibitors employed are summarized in Table 1, with the corresponding inhibitor structures shown in Figure 1.

MATERIALS AND METHODS

Three-dimensional structures of the complexes listed in Table 1 were retrieved from the Protein Data Bank.⁹ The development of our consensus molecular docking approach is based on QXP-Flo+0802.¹⁹ In addition to the full-MC method conventionally used as a searching algorithm in QXP, we have made use of the LMCS, which also is part of the QXP suite and which restricts rotational angles to smaller intervals, for example, between 20° and 30°, thereby limiting the conformational search space.

The consensus scoring method always starts with a full-MC run followed by a series of local-MC docking runs (LMCS run). The 25 results from an initial full-MC docking run, which are usually ranked by their E_{ass} , were further ranked according to additionally available parameters calculated by QXP. These are E_{nbd} , vdW, vdW+, E_{est} , E_{cnt} , and N_{hph} . Ranking was achieved by assigning a score of 1 to all those data of a given result which lie within a range of ± 2 of the best value (B_v) for the given parameter ($B_v \pm 2$).

The single scores were then summed up to the total score (S_{Total}). For instance, if E_{nbd} yields a lowest value of -35.6 in a given set of 25 docking answers, all those results from any of the other 24 docking answers that have E_{nbd} between

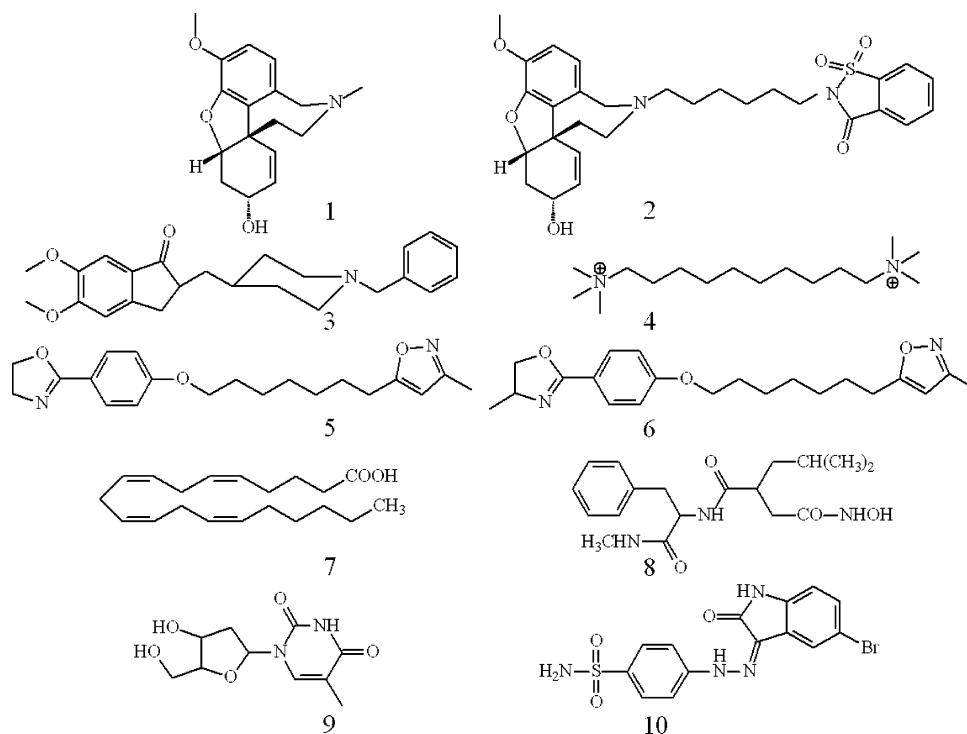


Figure 1. Structure of ligands used in the development and evaluation of the QXP-MSD approach: galanthamine (1), BHG (2), E2020 (3), decamethonium (4), WIN52711 (5), WIN52084 (6), arachidonic acid (7), methylamino-phenylalanyl-leucylhydroxamate (8), deoxythymidine (9), and oxindole (10).

−33.6 and −35.6, are also given a score of 1 for the E_{nbd} parameter. Positive numbers are treated similarly. The total score of each hit is calculated according to the following equation, in which individual S terms denote the scores for the particular parameters:

$$S_{\text{Total}} = S_{E_{\text{nbd}}} + S_{\text{vdW}} + S_{E_{\text{est}}} + S_{E_{\text{cnt}}} + S_{\text{vdW}+} + S_{N_{\text{hph}}}$$

$$0 \leq S_{\text{Total}} \leq 6$$

When, after an initial full-MC experiment, the docking result with the highest S_{Total} is not the one with the lowest E_{ass} , the highest-scoring structure is taken as the starting conformation for a first LMCS run,^{34,35} in which the rotational angle is varied between 20° and 30°. This limits the conformational search space and increases the probability of success in the random search and quickly removes atomic clashes between the ligand atoms and the receptor. This LMCS procedure is repeated with the resulting docking answers until the hit with the lowest E_{ass} also shows the highest S_{Total} . While the standard QXP procedure makes use of E_{ass} as the only criteria for ranking the docking results, the S_{Total} score is an ad hoc method employing various data output of interaction parameters calculated by the standard QXP force field.

E_{ass} , the total estimated binding energy, and LE, the ligand energy relative to the global minimum, are not considered in the calculation of S_{Total} . Nevertheless, they are most important for the identification of the final result of the multistep procedure because the final docking result is only reached when the highest S_{Total} is on the first rank, that is, when it also shows the lowest E_{ass} . At this point, one further docking step is always carried out to determine whether the best hit can still be optimized further to a lower-energy structure.^{33,48} The entire process of the QXP-MSD method is summarized in Figure 2.

To decrease the calculation time, the protein is kept rigid throughout the entire docking experiment, although there is no general limitation for the flexibility of the receptor active site in QXP-MSD. Because of the limitation of the number of atoms to less than 2000 in the QXP version employed, a spherical fraction of the proteins around the known binding site has been used for docking. In the case of acetylcholinesterase, this is a sphere with a radius of 17.0 Å around the hydroxyl oxygen of Tyr121; in the rhinovirus protein, it is a 17.0 Å radius sphere around the hydroxyl oxygen of Tyr197, and in the thymidine kinase, we used a 17.0 Å radius sphere around the hydroxyl oxygen of Tyr172. Polar hydrogen atoms were then added, followed by optimization of their positions. This subset of the protein was utilized for docking experiments which typically involved 10 000 cycles per run. The correctness and the quality of the docking results are checked by calculating the RMSD of the docking solution with respect to the coordination of the ligand in the X-ray structure.

RESULTS AND DISCUSSION

The development of QXP-MSD is described here for the reproduction of the inhibitor BHG (2; Table 1) complexed with AChE. The crystal structure of this complex will be published elsewhere.³⁷ The QXP-MSD method is driven by a consensus scoring that is based on energy criteria derived from QXP-docking experiments. BHG (2) consists of three main components, a demethylated galanthamine connected to a benzosulfonamide moiety via a hexyl spacer (Figure 1). The docking experiment is referred to as bound docking because it is performed on the known crystal structure of the AChE–BHG complex by extracting the inhibitor from the protein and docking it back into the binding site. The accuracy of the result is assessed by calculation of the RMSD

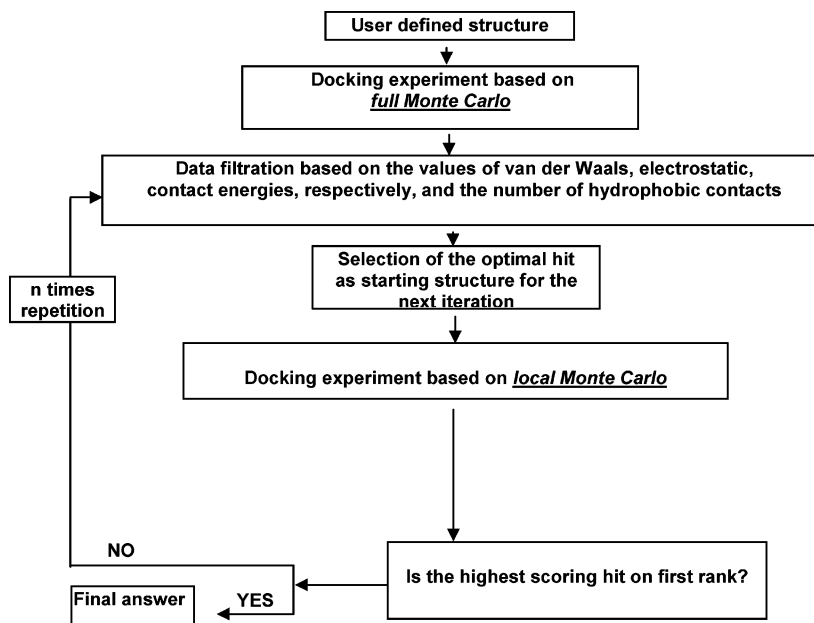


Figure 2. Schematic representation of the QXP-MSD procedure.

between the native, complexed structure of BHG (2) and the docking result.

The docking procedure always starts with a QXP docking run under full-MC conditions. The 25 structures resulting from this first experiment are then analyzed in terms of various energy and contact criteria. In particular, we take into account E_{ass} , LE, E_{nbd} , vdW, vdW+, E_{est} , E_{cnt} , N_{hph} , and the number of hydrogen bonds (N_{hyd}) (see Table 2). The usual ranking of the 25 docking answers in QXP is based on E_{ass} . However, the structure with the lowest E_{ass} value does not necessarily also have the best values for all of the other parameters. Therefore, all those structures that show the B_v in a given term of the various parameters as listed in Table 2 are given a score of 1. In addition, all those structures of the 25 docking answers that only deviate in a given term by two units or less ($B_v \pm 2$) from the best result are also given a score of 1. For instance, for E_{nbd} , the docking answer of rank 4 (see Table 2) shows the best value with -50.6 kJ/mol and, therefore, gets a score of 1 for this term. Then, any docking answer that has an E_{nbd} in the range of -50.6 to -48.6 kJ/mol also receives a score of 1 for this parameter. This applies, for instance, for the structures in rank 2 because it shows -50.1 kJ/mol. By this method, a given docking result can sum up more than one score point. Because N_{hyd} is quite often less than 3, N_{hyd} is not included in the calculation of S_{Total} .

The single scores of the 25 docking answers are then added to give the respective S_{Total} . If the structure with the highest S_{Total} is not in the first rank, this structure is used as the starting conformation for the next docking run, which is the first run under LMCS conditions with a restricted rotational angle (between 20° and 30°). If more than one structure has the same highest S_{Total} value, the one with the best rank is chosen for the next step.

As can be seen from Table 2, rank number 2 has the highest S_{Total} ($S_{\text{Total}} = 5$). The corresponding structure shows a RMSD of 0.60 Å as compared to 1.62 Å for the structure on the first rank. In the given case of Table 2, docking answer 2 is used as the starting structure for the next run, the first

LMCS run. The resulting 25 docking answers of that experiment are again analyzed according to the consensus scoring procedure described above. After an additional LMCS run, the first rank, that is, the one with the lowest E_{ass} , also shows the highest S_{Total} (see Table 3).

Application of the QXP-MSD procedure for the docking of BHG (2) into the corresponding AChE structure results in a final structure with a RMSD of 0.64 Å and, therefore, successfully reproduces the X-ray structure. The resulting structure is shown in Figure 3 (right) overlaid on the crystal structure. For comparison, the first docking answer, which resulted from the initial full-MC run with a RMSD of 1.62 Å (first rank of Table 2), is also shown (Figure 3, left).

It should be emphasized that only the MSD procedure allows the correct prediction of the orientation and conformation of the ligand in the binding site, while the standard QXP docking procedure yields a final solution (lowest E_{ass}) with a RMSD of 1.62 (see Table 2). In the given example, only one LMCS run is necessary, while in other cases, we had to perform more than 10 LMCS steps (see Figure 4). On the other hand, it is worth mentioning that the solution with the highest S_{Total} in the initial full-MC docking run already gives an acceptable conformation because it shows a RMSD of 0.60 (second rank of Table 2). The corresponding structure is virtually identical with the final docking solution (RMSD = 0.64 , see first rank of Table 3). However, both results show different energies with the final solution being the more stable conformation. Therefore, while the scoring procedure (S_{Total}) finds the correct ligand pose, the MSD regime drives this structure to rank 1, that is, to the one with lowest E_{ass} .

Comparison of the QXP-MSD Method in a Bound and Unbound Docking Experiment. When the crystal structure of a protein–ligand complex is not yet known, molecular docking procedures are the standard tools for a predicting the ligand placement in the binding site of a protein. In the case of AChE, a wealth of information is known about the crystal structure of various AChE-inhibitor complexes, which largely comes from the group of Sussman et al. (for recent

Table 2. Numerical Output of the First Step of the Bound Docking of BHG (2) Using the Full-MC Search Algorithm^a

Rank	RMSD	E _{ass}	LE	E _{nbd}	vdW	E _{est}	E _{cnt}	vdW+	N _{hph}	N _{hyd}	Score
1	1.62	-39.0	8.6	-47.6	-6.3	-8.4	-32.9	8.4	12	2	2
2	0.60	-38.3	11.9	-50.1	-12.6	0.1	-37.7	5.5	13	1	5
3	1.82	-37.1	10.2	-47.2	-9.9	-2.5	-34.7	6.1	13	3	2
4	1.39	-36.8	13.7	-50.6	-9.4	-6.2	-34.9	7.3	11	3	1
5	2.34	-36.3	8.7	-44.9	-7.9	-3.9	-33.1	7.7	11	2	0
6	0.69	-36.1	8.5	-44.5	-9.3	-1.4	-33.7	6.7	12	2	2
7	1.31	-35.8	12.5	-48.2	-8.0	-8.2	-32.0	6.6	13	2	3
8	1.67	-34.7	14.7	-49.3	-9.8	-3.8	-35.8	7.2	12	2	4
9	1.52	-34.7	9.8	-44.4	-4.4	-7.4	-32.6	11.0	12	3	1
10	1.81	-34.5	9.2	-43.8	-3.7	-5.1	-35.0	13.3	9	2	0
11	1.16	-34.4	9.5	-43.9	-7.8	-6.1	-30.1	6.2	13	2	2
12	1.53	-34.2	13.3	-47.6	-3.2	-9.5	-34.8	13.5	11	3	1
13	0.81	-34.2	9.2	-43.3	-8.8	-1.7	-32.9	5.9	11	2	1
14	2.39	-34.0	7.9	-41.8	-4.6	-4.4	-32.8	10.3	13	2	1
15	1.59	-33.8	11.1	-45.0	-6.5	-5.8	-32.7	8.6	12	2	1
16	0.93	-33.7	7.0	-40.6	-9.2	0.9	-32.3	6.0	12	2	2
17	0.79	-33.6	12.5	-46.1	-12.0	0.7	-34.8	5.2	14	1	3
18	0.94	-33.4	12.1	-45.5	-9.7	-3.1	-32.7	5.3	14	2	2
19	0.84	-33.4	11.3	-44.9	-10.0	0.5	-35.4	7.4	11	1	0
20	1.75	-33.4	12.8	-46.1	-7.0	-5.4	-33.7	8.4	13	2	1
21	0.98	-33.3	8.3	-41.4	-9.3	0.0	32.1	5.8	2	1	1
22	1.97	-33.3	16.1	-49.3	-11.3	-2.3	-35.7	6.3	11	2	4
23	0.74	-33.3	13.0	-46.2	-8.2	-0.3	-37.7	9.5	13	1	2
24	1.85	-33.2	8.7	-41.9	-5.4	-6.2	-30.3	7.8	8	2	0
25	1.34	-33.2	11.4	-44.6	-9.4	-2.6	-32.6	5.8	12	1	2

^a Rank number 2 shows the highest S_{Total} with a score of 5. The best values (B_v) for each column each yield a score of 1 (red numbers). Furthermore, all those values that fall into the range of $B_v \pm 2$ of the corresponding column also score one additional point (blue numbers). S_{Total} is summed up from the single scores (of the gray formatted fields) of all 25 docking answers. RMSD: root-mean-square deviation (Å). E_{ass} : total estimated binding energy (kJ/mol). LE: conformation energy of the ligand (kJ/mol). vdW: van der Waals energy (kJ/mol). vdW+: positive van der Waals energy (kJ/mol). E_{est} : electrostatic energy (kJ/mol). E_{cnt} : contact energy of interactions (kJ/mol). E_{nbd} : total energy of nonbonded interactions (kJ/mol). N_{hph} : number of hydrophobic contacts. N_{hyd} : number of hydrogen bonds. Score: total score of each hit (S_{Total}). N_{hyd} is not included in the calculation of S_{Total} .

publications, see refs 49 and 50), with additional structures from the groups of Lamba et al.³⁸ and Bourne et al.⁵¹ As of February 2006, the PDB database contained a total of 61 AChE structures.

Because of the large amount of PDB entries for AChE, one can choose a suitable AChE structure for the docking experiments according to similarities between the ligand under investigation and known crystal structures of inhibitors. In this respect, PDB entry 1EVE,⁴⁰ which describes the complex of TcAChE with E2020 (3), seems to be an appropriate choice for unbound docking because BHG (2) can be expected to bind to the AChE gorge in a similar way, that is, in a stretched conformation.

A full-MC run with BHG (2) into AChE structure 1EVE resulted in 25 answers, the fifth of which gave the highest S_{Total} (Table 4). The RMSD of this structure is 0.77 Å as compared to 1.72 Å for the first rank. Starting from the fifth-ranked structure, a total of 11 QXP-MSD steps were necessary to finally yield the structure with the highest S_{Total} on first rank (Table 5). The resulting structure shows a RMSD of 0.76 Å. A comparison of the first rank of Tables

4 and 5 with the crystal structure of BHG (2) is shown in Figure 5. One can see that the difference is largely due to the positioning of the saccharino system, which is bound to the galanthamine core by a hexamethylene spacer. Because of the limited space available at the bottom of the gorge, the galanthamine ring system shows up in almost the same location and conformation in all of the docking answers. This is a general finding with all structurally investigated galanthamine-based inhibitors of AChE (data not shown).

The course of the E_{ass} and of the LE during the 13 steps of the unbound QXP-MSD experiment of docking BHG (2) into 1EVE⁴⁰ is shown in Figure 4 along with the corresponding rank of the highest S_{Total} -scoring docking answer.

As can be seen from this figure, docking run 9, which after the initial full-MC search is the eighth MSD run, already yields a first rank that also has the highest S_{Total} . Because the resulting structure is not of zero ligand energy (LE of this docking solution is 6.1 kJ/mol), the procedure is continued to check if the ligand structure still can be improved. The next docking run, however, yields the highest S_{Total} for the solution on rank 5 rather than for the first rank,

Table 3. Numerical Output of the QXP-MSD Docking of BHG (2) after the Final LMCS Run^a

Rank	RMSD	E _{ass}	LE	E _{nbd}	vdW	E _{est}	E _{ent}	vdW+	N _{hph}	N _{hyd}	Score
1	0.64	-57.7	6.6	-64.3	-10.4	-15.8	-38.1	7.7	14	3	5
2	1.64	-56.0	5.9	-61.9	-5.6	-23.0	-33.3	9.0	15	3	2
3	1.82	-54.5	7.5	-62.0	-8.5	-18.6	-34.9	7.8	15	4	3
4	0.57	-54.5	9.3	-63.8	-10.2	-15.4	-38.2	8.4	14	2	5
5	0.79	-54.0	6.4	-60.4	-10.2	-13.7	-36.5	7.3	15	2	4
6	1.39	-53.8	10.3	-64.2	-9.2	-19.7	-35.3	7.7	13	4	4
7	1.31	-53.6	9.5	-63.1	-5.7	-24.9	-32.5	9.1	14	3	4
8	1.47	-53.6	7.6	-61.2	-4.3	-25.0	-31.8	9.7	15	3	2
9	1.55	-53.5	10.0	-63.6	-4.5	-25.8	-33.3	11.1	15	3	3
10	0.71	-53.3	5.5	-58.8	-7.5	-17.2	-34.1	8.5	12	3	1
11	1.58	-52.9	7.6	-60.4	-4.3	-23.5	-32.7	10.8	13	3	1
12	1.59	-52.8	9.4	-62.2	-2.4	-23.9	-35.9	14.9	12	3	1
13	1.25	-52.7	10.0	-62.6	-7.1	-22.7	-32.8	7.9	15	3	3
14	1.31	-52.5	6.2	-58.7	-6.3	-20.3	-32.0	8.8	13	3	2
15	1.77	-51.9	10.2	-62.1	-4.2	-23.8	-34.1	11.6	15	4	2
16	0.72	-51.9	5.2	-57.1	-6.7	-16.6	-33.8	8.3	13	2	2
17	1.45	-51.9	6.7	-58.6	-4.0	-22.4	-32.2	10.9	14	4	1
18	1.2	-51.7	9.4	-61.1	-5.9	-22.6	-32.6	9.5	14	3	1
19	0.86	-51.6	6.2	-57.8	-5.7	-18.5	-33.6	9.2	12	3	1
20	2.41	-51.5	4.7	-56.3	-1.2	-21.3	-33.7	13.7	14	3	1
21	1.69	-51.3	12.4	-63.8	-8.6	-18.9	-36.3	8.5	14	3	5
22	0.86	-51.3	5.9	-57.2	-9.9	-10.7	-36.6	7.5	13	2	4
23	2.04	-51.2	11.2	-62.4	-3.4	-25.8	-33.2	11.7	12	4	2
24	1.86	-51.0	11.5	-62.5	-5.3	-21.1	-36.1	12.0	15	3	2
25	1.43	-50.9	7.3	-58.2	-3.4	-23.0	-31.8	11.1	13	3	1

^a The first rank shows the highest S_{Total} with a score of 5. For further details, see Table 2.

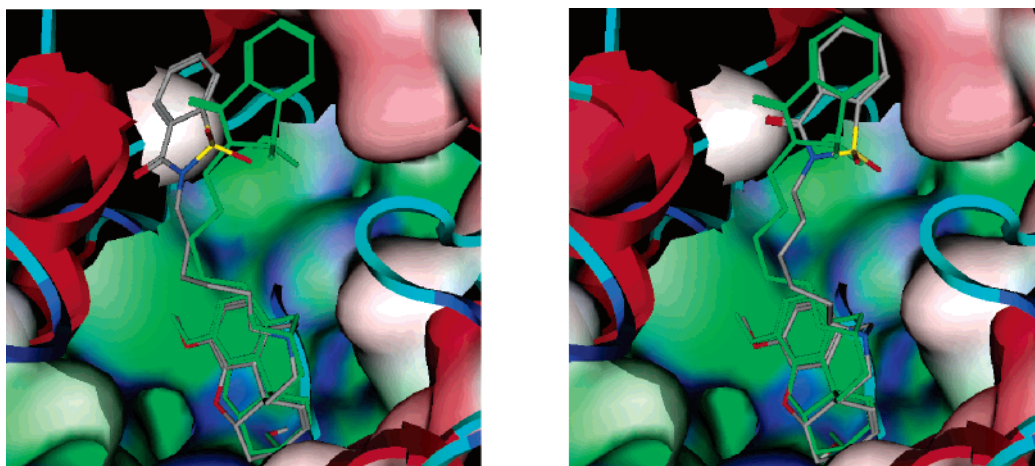


Figure 3. Left: Structural overlay of the BHG-AChE crystal structure (green) with the first rank from a conventional QXP (full MC) docking procedure (gray). Right: Final answer from the QXP-MSD procedure with a RMSD of 0.64 Å (gray), overlaid on the crystal structure (green).

so the docking process is continued. It turns out that in the next docking answer (run 11), the highest S_{Total} is back on the first rank, the corresponding structure of which then can be further improved to $LE = 0$, yielding the final answer in the 12th run. Continuation of the docking experiment does not improve the results. This series of docking runs demonstrates that it is always advisable to do at least one additional docking experiment, when the highest S_{Total}

solution is on the first rank but does not show zero ligand energy. We have, however, encountered many results in which the final ligand energy is not equal to 0 kJ/mol. In these structures, the remaining internal ligand energy is probably compensated by favorable interactions with surrounding amino acids of the binding site.

QXP-MSD Method Versus Multiple Use of First Rank from MSD Runs. To study the effect of the starting

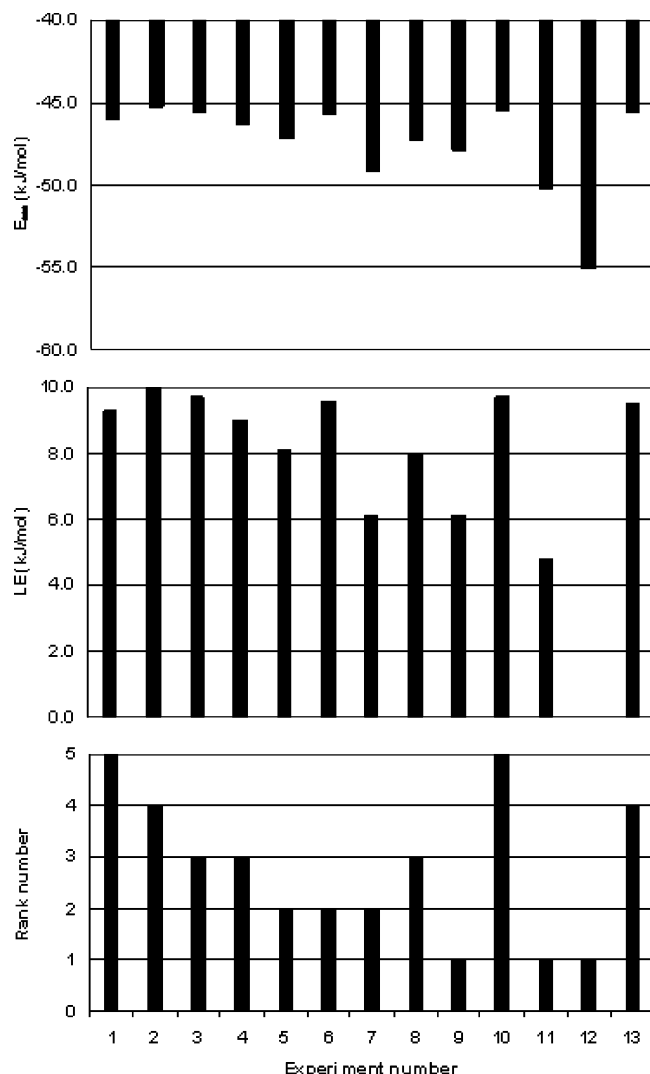


Figure 4. Variation of total estimated binding energy (E_{ass}), and ligand energy (LE), with the corresponding rank number of the highest S_{Total} as resulting from the unbound multistep docking of BHG (2) into 1EVE.⁴⁰ The optimal result was obtained in the 12th docking step.

conformation in the QXP-MSD procedure, we have compared the results from the bound docking experiment of BHG (2) with those of a procedure in which the first hit of a previous experiment was always used for the next step, rather than the docking answer with the highest S_{Total} . Again, this experiment was run until the first hit, that is, the one with the best E_{ass} , also showed the highest S_{Total} employing BHG (2) under unbound docking conditions with 1EVE⁴⁰ as an AChE template. The results are given in Table 6, demonstrating that the QXP-MSD procedure not only gives the better RMSD but also has the higher S_{Total} .

The MSD experiment, therefore, is preferred over an MSDF procedure. It yields better energy data as well as a better RMSD value. In fact, the final answer reached in the MSDF experiment would not result in an acceptable structure because it shows a RMSD of 1.63 Å. Thus, increasing the number of steps in a multistep docking procedure is not the only determining argument. Rather than always using the docking answer with the lowest E_{ass} , one has to employ the answer with the highest S_{Total} until the docking solution with highest S_{Total} also shows the lowest E_{ass} .

Importance of Choosing the Correct Protein Template for the Correct Prediction of a Ligand Structure. To study the effect of the selection of a suitable X-ray structure of a protein for unbound docking, we have compared the data of the previous experiment that uses 1EVE⁴⁰ with results from docking BHG (2) into two additional crystal structures independently published for the AChE–galanthamine complex, 1DX6³⁹ and 1QTI.³⁸ In contrast to 1EVE, in which the ligand E2020 covers most of the AChE gorge, the ligand galanthamine in 1DX6 and 1QTI only binds to the lower part of the gorge. Additionally, we have investigated the influence of the conformation of the nitrogen-bound side chain of BHG (2), which in the starting structure was either axially or equatorially attached to the seven-membered-ring nitrogen of the galanthamine core.

The results as shown in Table 7 demonstrate that, with all three protein templates, the axial starting conformation of BHG (2) gives the better energy. However, only one template, the AChE protein from 1EVE, yields the correct answer with a RMSD of 0.76 Å. Neither 1DX6 nor 1QTI yield an appreciable solution, despite the fact that the 1QTI experiment gives a final docking answer with a RMSD of 0.85 Å. Visual inspection of the corresponding structure discloses an inverted orientation of the benzosulfimido ring with respect to the crystal structure (see Figure 6). The RMSD of 0.85 Å is a result of the strong similarity of the correct complex structure and the final solution of the 1QTI docking run. The inverted benzosulfimido ring does not give rise to a large increase in RMSD because of the pseudo-symmetry in which only the CO and the SO₂ groups are exchanged.

The data in Table 7 clearly demonstrate the importance of picking the appropriate starting structure in the case of an unbound docking experiment. Small changes in orientation of the amino acid side chains in 1EVE as compared to the corresponding ones of 1DX6 and 1QTI seem to be responsible for the different docking results. In 1EVE, similarly to the AChE–BHG complex, the ligand is stretched along the entire gorge, from the lower to the upper part. In both structures, a Trp279 at the mouth of the gorge plays a key role in accommodating part of the ligand by anchoring to an aromatic residue. Unless a flexible docking regime is used that allows protein side chains to bind to the ligand by induced fit, a docking experiment employing a rigid protein can only yield the correct answer if an appropriate starting structure with respect to the orientation of the amino acid side chains of the binding site is used. Therefore, in an unbound docking experiment, one would always prefer to start from a variety of unliganded complexes of the respective protein, including the apo structure, to sample the structural variation of the binding site. In this respect, it should be noted that the galanthamine core structure of BHG (2) does show up in a very similar orientation in the 1DX6- and 1QTI-docking experiment (see Figure 6), which, in addition, is almost identical to the orientation and conformation of galanthamine in the corresponding 1DX6 and 1QTI complexes, respectively.

QXP-MSD Versus the Simulated Annealing Procedure. The results of QXP-MSD docking of BHG (2) have further been compared to an unbound simulated annealing experiment utilizing 1EVE as a protein scaffold. For this purpose, the docking answer with the highest S_{Total} from an initial

Table 4. Numerical Output of the First Step of the Unbound Docking of BHG (2) in 1EVE⁴⁰ Using the Full-MC Search Algorithm^a

Rank	RMSD	E _{ass}	LE	E _{mbd}	vdW	E _{est}	E _{ent}	vdW+	N _{hph}	N _{hyd}	Score
1	1.72	-48.8	5.2	-53.9	4.3	-21.1	-37.1	20.3	14	2	2
2	1.51	-47.7	9.0	-56.3	-1.9	-16.4	-38.0	15.3	13	3	4
3	0.88	-46.2	3.3	-49.6	-1.0	-13.6	-35.0	13.8	11	2	1
4	1.62	-46.0	6.2	-52.2	4.5	-19.9	-36.9	20.9	14	2	2
5	0.77	-46.0	9.3	-55.3	-3.8	-12.0	-39.5	14.5	15	2	5
6	1.35	-45.9	10.6	-56.5	-1.1	-18.3	-37.1	15.8	13	3	2
7	1.72	-45.9	6.3	-52.2	0.7	-15.7	-37.2	17.6	13	3	1
8	1.87	-45.8	7.2	-53.0	-3.0	-15.1	-34.9	13.1	11	2	2
9	1.64	-45.3	5.5	-50.8	5.2	-19.9	-36.1	21.3	13	3	2
10	0.93	-45.2	5.5	-50.7	-1.5	-11.2	-37.9	16.1	12	1	1
11	0.73	-45.1	5.4	-50.4	-2.3	-12.5	-35.6	14.4	11	2	2
12	0.71	-45.0	8.5	-53.5	-0.2	-14.5	-38.8	17.1	15	1	2
13	1.33	-44.5	8.2	-52.7	2.8	-19.7	-35.8	19.0	13	3	2
14	1.38	-44.4	4.3	-48.7	1.3	-14.3	-35.7	17.1	12	3	0
15	1.49	-44.4	7.3	-51.7	5.1	-21.1	-35.7	20.6	13	2	2
16	1.09	-44.2	7.9	-52.1	-3.7	-9.5	-39.0	14.0	13	3	4
17	1.54	-44.0	7.2	-51.2	4.4	-18.6	-37.0	21.0	13	2	1
18	1.46	-43.5	9.0	-52.6	-3.2	-15.9	-33.5	13.0	12	3	2
19	1.56	-43.0	6.6	-49.6	1.3	-14.3	-36.5	17.6	14	3	1
20	1.25	-42.9	4.5	-47.5	-0.2	-11.6	-35.6	15.7	11	3	0
21	0.96	-42.6	4.1	-46.7	-1.6	-12.5	-32.6	12.9	11	2	1
22	1.74	-42.5	6.4	-48.9	2.9	-15.5	-36.3	20.1	12	2	0
23	1.32	-42.4	5.4	-47.8	0.1	-12.4	-35.6	15.5	12	3	0
24	1.03	-42.3	4.3	-46.6	0.5	-10.9	-36.2	16.6	13	3	1
25	1.01	-42.3	5.7	-48.1	-0.1	-13.5	-34.5	15.1	9	3	0

^a Rank number 5 shows the highest S_{Total} with a score of 4. For further details, see Table 2.

full-MC search (fifth rank in Table 4) was docked into the flexible binding site of 1EVE. The annealing temperature and flat-well radius (the allowed radius for the movement of amino acids in the binding site) were carefully defined in order to trap the ligand in a good minimum.⁴⁶ Therefore, four individual docking runs with different starting temperatures were performed at 600, 500, 400, and 300 K to find the optimal highest temperature. Starting with a flat-well radius of 0.1 Å, the system was cooled to 30 K.

The results of these experiments (Table 8) show that the highest S_{Total} was obtained with an annealing temperature of 600 K. The resulting structure has the best E_{ass} , the highest S_{Total} , and, at the same time, the best RMSD (0.85 Å). A further increase in temperature probably does not improve the result, as an annealing temperature of 500 K already gives a quite acceptable solution. In addition, a smaller flat-well radius of 0.1 Å proved to be more favorable than a radius of 0.2 Å (Table 8).

It should be noted, however, that the simulated annealing experiment similar to docking BHG (2) into 1QTI also yields an inverted benzosulfimido ring. The docking of BHG (2) under these conditions does not yield a correct answer and, therefore, cannot compete with the quality and correctness of the results from QXP-MSD experiments.

Further Evaluation of the QXP-MSD Procedure. To assess the multistep docking process for other AChE-inhibitor

complexes, and for other protein–ligand complexes in general, we have performed a series of experiments that allow us to judge the scope and limitation of the QXP-MSD method.

In particular, we have docked (a) the flexible ligands E2020 (3), decamethonium (4), WIN51711 (5), WIN52084 (6), arachidonic acid (8), and methylamino-phenylalanyl-leucyl-hydroxamat (9) as well as (b) the ligands deoxythymidine (7) and oxindole (8), which have less-flexible structures.

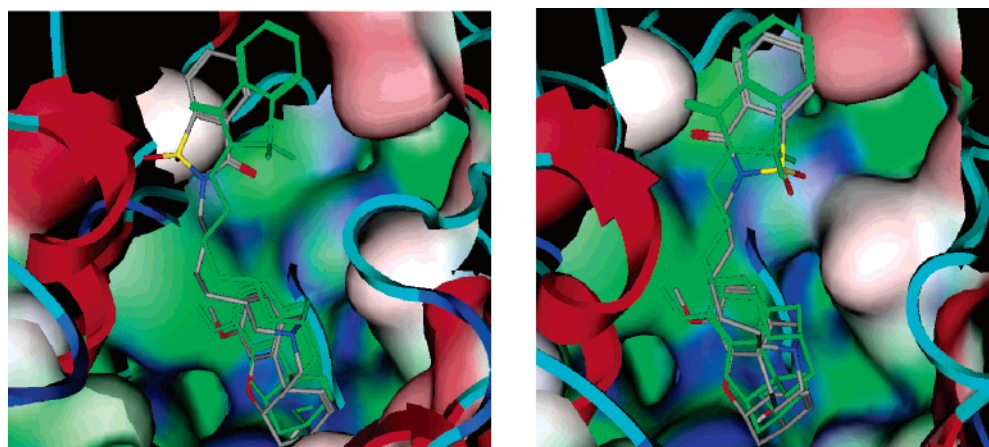
E2020 (3), an AChE inhibitor also known as donepezil,⁴⁰ is a potent drug for the treatment of Alzheimer's disease. It is used as a racemat, but when the crystal structure of the AChE–E2020 complex was investigated, only the R enantiomer was found to bind to the active site, which is well in line with the better activity of this stereoisomer.⁴⁰ Early attempts to predict the crystal structure of the AChE–E2020 complex did not give an unequivocal answer but, rather, favored an upside-down orientation of the ligand in the gorge.⁵² We have used the AChE templates from the galanthamine (1) complex (1DX6³⁹) as well as from the decamethonium (4) complex (1ACL⁴¹) to predict the binding mode of E2020 in the AChE complex in unbound docking experiments.

Full-MC docking starting from the AChE structure from 1DX6 yields a first-ranked structure with a RMSD of 2.19

Table 5. Numerical Output of the Unbound QXP-MSD Docking of BHG (2) in 1EVE⁴⁰ after the Final LMCS Run^a

Rank	RMSD	E _{ass}	LE	E _{nbd}	vdW	E _{est}	E _{cnt}	vdW+	N _{nph}	N _{hyd}	Score
1	0.76	-55.1	0.0	-55.1	-3.4	-12.1	-39.6	14.7	14	2	4
2	0.73	-50.4	0.0	-50.4	-2.5	-12.5	-35.4	14.0	11	2	1
3	1.73	-48.9	5.0	-53.9	4.3	-21.1	-37.1	20.3	14	3	2
4	1.50	-47.8	8.8	-56.6	-2.3	-16.8	-37.5	14.8	13	4	3
5	1.80	-46.2	6.3	-52.5	1.4	-16.0	-37.9	18.5	13	3	1
6	1.32	-45.9	10.3	-56.3	-1.0	-18.1	-37.1	15.9	13	3	2
7	0.87	-45.9	3.4	-49.3	-0.4	-14.1	-34.8	14.2	11	2	0
8	1.86	-45.9	7.0	-52.9	-3.2	-15.1	-34.6	12.6	11	2	2
9	1.24	-45.0	8.7	-53.8	0.4	-17.5	-36.6	17.1	14	3	1
10	0.74	-44.8	4.3	-49.1	-1.9	-12.9	-34.3	13.6	11	2	1
11	0.88	-44.5	5.8	-50.3	-1.2	-10.7	-38.5	16.5	14	2	2
12	1.40	-44.4	4.5	-48.9	1.8	-15.0	-35.7	17.7	12	3	0
13	1.60	-44.4	7.1	-51.5	1.1	-15.4	-37.1	17.9	13	4	1
14	1.44	-44.2	8.0	-52.2	-4.3	-14.8	-33.2	11.6	12	3	2
15	1.51	-44.0	7.2	-51.2	4.0	-18.3	-36.9	20.6	13	2	1
16	1.91	-43.9	8.5	-52.4	-3.0	-14.7	-34.8	12.9	11	3	2
17	1.33	-43.9	8.1	-51.9	4.2	-21.0	-35.2	19.9	14	3	2
18	1.05	-43.4	8.0	-51.4	-0.7	-13.7	-37.0	16.2	13	3	1
19	1.30	-42.7	9.2	-51.8	3.3	-19.6	-35.6	19.3	15	3	2
20	1.43	-42.5	7.0	-49.6	5.8	-19.8	-35.5	21.4	14	3	2
21	1.32	-42.5	7.0	-49.5	-3.2	-13.6	-32.7	12.2	12	2	2
22	0.92	-42.5	7.3	-49.8	-0.4	-11.5	-37.9	16.2	14	1	1
23	1.03	-42.4	4.3	-46.8	-0.1	-10.2	-36.4	16.5	13	3	1
24	1.67	-42.4	6.8	-49.1	-1.1	-11.4	-36.7	14.8	13	2	1
25	0.94	-42.3	11.1	-53.4	-1.4	-11.9	-40.1	16.9	14	2	2

^a Rank number 1 is the optimal hit with the highest S_{Total} (score of 4). For further details, see Table 2.

**Figure 5.** Overlay of the BHG (2) crystal structure (green) with the first ranked answer of a one-step full-MC docking of BHG (2) into 1EVE⁴⁰ (left, colored in gray) and the finally predicted BHG (2) structure obtained after 11 LMCS steps (right, gray), respectively.

Å as compared to the crystal structure, while rank number 9 shows the highest S_{Total} with a RMSD of 0.97 Å (Table 9). All of the 25 QXP answers of this experiment are similarly placed in the gorge because they all show the same “right-side-down” orientation with respect to the gorge axis. QXP-MSD docking, starting from the highest S_{Total} hit of the full-MC run, then leads to a final answer with a RMSD of 0.96 Å. As is generally the case, the structure finally resulting

from the QXP-MSD experiment has a lower E_{ass} than that of the first hit from the first full-MC run.

If 1ACL is used as an AChE template, the QXP-MSD procedure also generates the correct solution for the E2020 structure with a RMSD of 0.92 Å (Table 9). Again, the protein crystal structure used in these docking experiments obviously is preformed for hosting the ligand E2020 (3).

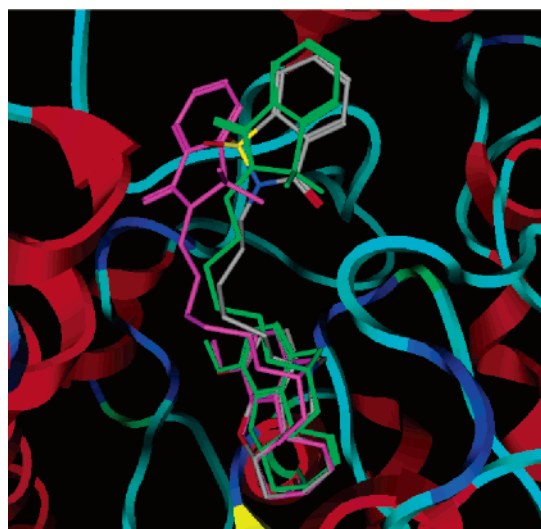
Table 6. Multistep Docking Experiment Always Using the First Rank as the Starting Structure for the Next Docking Run (QXP-MSDF), Compared to the Procedure as Described in Tables 2 and 3, That Is, When Starting from the Highest S_{Total} Hit (QXP-MSD)^a

Experiment	RMSD	E _{ass}	LE	E _{nbd}	vdW	E _{est}	E _{cnt}	vdW+	N _{hph}	N _{hyd}	Score	Number of steps
QXP-MSDF	1.63	57.1	4.8	61.9	-5.5	23.2	-33.1	9.2	15	2	2	6
QXP-MSD	0.64	57.7	6.6	64.3	-10.4	15.8	-38.1	7.7	14	3	4	6

^a For further details, see Table 2.**Table 7.** Numerical Output of the Final Result from the Unbound QXP-MSD Docking of BHG (2) in 1EVE,⁴⁰ 1DX6,³⁹ and 1QTI^{38 a}

protein	RMSD	E _{ass}	LE	E _{nbd}	vdW	E _{est}	E _{cnt}	vdW+	N _{hph}	N _{hyd}	alkyl chain	saccharine
1QTI	0.85	-60.2	1.2	-61.4	-14.1	-10.7	-36.6	3.9	15	1	a	inverted
1QTI	1.94	-55.6	4.3	-59.8	-8.7	-15.4	-35.8	8.9	9	3	e	off
1DX6	1.79	-64.3	3.9	-68.2	-6.7	-23.8	-37.8	11.5	12	3	a	off
1DX6	2.15	-60.7	4	-64.7	-8.1	-18.6	-38.1	10.0	13	3	e	off
1EVE	0.76	-55.1	0	-55.1	-3.4	-12.1	-39.6	14.7	14	2	a	correct
1EVE	3.07	-50.1	0.9	-51.0	-4.1	-16.5	-30.4	10.5	9	2	e	off

“alkyl chain” depicts the conformation of the N-alkyl chain; “saccharine” denotes the orientation of the saccharine ring with respect to the crystal structure of BHG (2). For further details, see Table 2.

**Figure 6.** Overlay of BHG (2) structure as predicted in unbound docking experiments with 1DX6 (magenta) and 1QTI (gray) on the X-ray structure (green). Note the inverted benzosulfimido ring in the 1QTI result.

These results must be due to a close structural similarity of the binding sites between these two templates, that is, the unbound AChE from 1DX6 and 1ACL. A structural inspection of the binding sites discloses that the most notable difference is the orientation of the swinging gate (Phe330), responsible for opening and closing the access to the gorge. But even this amino acid is almost identically placed in both AChE structures, so that there are only small differences between the centroid of Phe330 and the oxygen atom of Tyr121, being 8.64 Å in 1EVE, 8.81 Å in 1DX6, and 8.31 Å in 1ACL. In contrast, if the AChE template from the tacrine complex is used (1ACJ), E2020 cannot successfully be docked because the swinging gate in this structure is closed so that there is not room enough for the ligand to stretch out in the gorge. In this case,

the distance between the centroid of Phe330 and the oxygen atom of Tyr121 amounts to 5.99 (data not shown). This again demonstrates that the docking result depends to a large extent on choosing the appropriate structure to begin with. Only then can a suitable docking and scoring regime yield the correct result. This shortage, however, might be overcome by using a flexible docking procedure.

While E2020 (3) only has a few rotatable bonds, decamethonium (4) with its 11 single bonds between the two trimethylammonium groups probably is the most challenging AChE ligand for a docking experiment. Decamethonium (4) also differs from the other ligands utilized in this study because it is doubly charged. On the basis of the experiments with E2020 (3), we have used 1DX6³⁹ as the template for the unbound docking of 4 into AChE. As can be seen from Table 9, the full-MC docking run already yields a highest S_{Total} solution on the first rank (1 step 1) with an acceptable RMSD of 1.27 Å. If the QXP-MSD procedure is still applied, no structural refinement but rather an identical solution is obtained. Yet, the total estimated binding energy is improved by 8 kJ/mol, which entirely comes from the numerical comparison of the ligand energy in the bound state to the local minimum energy, obtained in the gas phase prior to the docking run.

The complex of a rhinovirus 14 protein with the antiviral compounds WIN51711 (5)⁴² and WIN52084 (6)⁴³ is an illustrative example for a rather unexpected ligand pose. The crystal structures of these complexes have revealed that the two ligands bind with reversed orientation in the rhinovirus active site, despite the very minor difference of only one extra methyl group in WIN52084 (7) with an otherwise identical structure to WIN52084. The docking of these two ligands, therefore, represents a nice challenge for our QXP-MSD method.

In the investigation of these two ligands, we have started with a bound docking experiment of WIN52084 into 1RUH

Table 8. Numerical Output from Simulated Annealing Experiments with BHG (2) and the AChE Structure from 1EVE⁴⁰ with Varying Annealing Temperatures and Flat-Well Radii^a

Flat-well (Å)	Temp (K)	RMSD	E _{ass}	LE	E _{nbd}	vdW	E _{est}	E _{cnt}	vdW+	N _{hph}	N _{hyd}
0.1	300	1.9	-59.2	8.5	-67.8	-9.9	-20.6	-37.4	9.5	14	3
0.1	400	1.85	-59.8	9.2	-68.6	-7	-24.7	-36.9	10.6	13	3
0.1	500	0.88	-60.3	9.2	-69.7	-12.4	-18.3	-39	6.1	16	2
0.1	600	0.85	-60.6	9.1	-70	-12.5	-18.4	-39	6.4	16	2
0.2	600	1.89	-65.2	9	-70.9	-7.8	-24.7	-38.4	10.5	13	3

^a For further details, see Table 2.**Table 9.** Numerical Output from Docking Experiments of Various Inhibitors^a

ligand/protein	rank/no. of steps	RMSD	E _{ass}	LE	E _{nbd}	vdW	E _{est}	E _{cnt}	vdW+	N _{hph}	N _{hyd}
E2020/1DX6	1 step 1	2.19	-38	3.2	-41.2	-9.5	-4.4	-27.3	3.6	13	1
E2020/1DX6	9 step 1	0.97	-37	9.4	-46.4	-11.9	-3.7	-30.7	3.2	12	1
E2020/1DX6	1 step 3	0.96	-41.6	4.1	-45.7	-11.8	-3.6	-30.4	3	12	1
E2020/1ACL	1 step 1	0.92	-44.7	4.4	-49.1	-10.2	-11.7	-27.2	3.9	11	0
E2020/1ACL	2 step 1	1.04	-43.5	4.8	-48.3	-11.2	-10.1	-27.1	3.1	11	0
E2020/1ACL	1 step 2	0.92	-44.8	4.4	-49.2	-10.2	-11.7	-27.3	4	11	0
decamethonium/1DX6	1 step 1	1.27	-27.5	8.7	-36.2	-8.8	-6.4	-21	1.7	7	0
decamethonium/1DX6	1 step 2	1.27	-35.5	0.7	-36.2	-8.8	-6.4	-21	1.6	7	0
WIN51711/1RUH	1 step 1	1.10	-44.3	2.3	-46.6	-11.9	-0.7	-34	4	13	0
WIN51711/1RUH	2 step 1	0.80	-44.1	2.9	-46.9	-13.3	-0.1	-33.6	3.3	12	0
WIN51711/1RUH	1 step 2	0.80	-46.9	0	-46.9	-13.3	-0.1	-33.6	3.3	12	0
WIN52084/1RUH	1 step 1	1.66	-47.2	1.7	-48.9	-13.5	-2.1	-33.3	3.6	12	1
WIN52084/1RUH	1 step 4	1.06	-48.9	0	-48.9	-13.2	-2.5	-33.2	3.7	12	1
arachidonic acid/1DIY	1 step 1	1.24	-63.3	0	-64.1	2.4	-37.0	-29.4	16.3	15	1
arachidonic acid/1DIY	2 step 1	1.17	-63.0	2.5	-66.3	1.8	-36.5	-31.7	16.6	14	1
arachidonic acid/1DIY	1 step 4	1.17	-66.0	0	-67.4	0.8	-36.5	-31.6	15.6	14	1
methylamino-phenylalanyl-leucyl-hydroxamate/1MNC	1 step 1	0.64	-40.9	13.8	-56.6	2.7	-41.7	-17.6	12.5	5	6
methylamino-phenylalanyl-leucyl-hydroxamate/1MNC	1 step 8	0.64	-47.1	7.6	-56.6	2.6	-41.7	-17.5	12.3	5	6
deoxythymidine/1KI6	1 step 1	0.43	-56.2	3.9	-60.1	-3.1	-36.4	-20.6	7.8	2	3
deoxythymidine/1KI6	1 step 2	0.74	-59.1	2.5	-61.6	2.5	-42	-22.1	13.7	1	3
deoxythymidine/1KI7	1 step 1	1.82	-44.8	5.1	-49.9	0.7	-29.2	-21.4	12	2	2
deoxythymidine/1KI7	1 step 4	1.11	-50.1	11	-61	14.4	-54.5	-21	23.6	2	3
deoxythymidine/1KI8	1 step 1	0.59	-47.0	9.4	-56.4	-6.4	-28.4	-21.6	5.3	2	5
deoxythymidine/1KI8	1 step 5	0.60	-51.3	1.7	-53	-5.6	-27.1	-20.3	5.2	2	4
oxindole/1FVT	1 step 1	0.46	-39.3	6	-45.3	2.8	-26.7	-21.4	13.4	6	5
oxindole/1FVT	1 step 5	0.45	-42.1	4.2	-46.3	3.1	-28.1	-21.4	13.6	6	6

^a For further details, see Table 2. "rank/no. of steps" defines the particular result, e.g., "9 step 1" stands for the 9th rank in the 1st docking step.

followed by an unbound docking of WIN51711 again into 1RUH, to find out if the QXP-MSD procedure can correctly predict the completely different placement of these two ligands in the rhinovirus protein bindings site.

As can be seen from Table 9, the first docking step (full MC) of the bound docking experiment with WIN52084 using its corresponding protein from 1RUH⁴³ yields a RMSD of 1.66 Å, with highest S_{Total} already on the first rank. Continuation of the docking run with three further LMCS steps finally results in an improved RMSD of 1.06 Å.

When the same protein is used to dock WIN51711, the first full-MC search yields the solution with highest S_{Total} on the second rank, which can be brought to the first rank by one further LMCS run. The final structure with a RMSD of 0.80 Å is identical to that of the highest S_{Total} of the first full-MC run and only differs by 2.6 kJ/mol of internal LE.

Arachidonic acid (7), a long stretched molecule with 15 rotatable bonds, is bound by the enzyme cyclooxygenase (COX) in order to be ultimately converted to prostaglandines. We have used the complex of COX-1 with arachidonic acid

(7)⁴⁴ (1DIY) in a bound docking experiment to predict this complex with our QXP-MSD method. Table 9 shows that the structure with the highest S_{Total} is found on rank number 2 and is structurally related to the first rank. Three further LMCS steps are necessary to drive the highest S_{Total} structure to rank 1, while maintaining an equally good structural similarity to the crystal structure (RMSD = 1.17 Å).

As a final example of a flexible ligand, we have used a peptide ligand to check the QXP-MSD method for its reproducibility. The ligand methylamino-phenylalanyl-leucyl-hydroxamate (8) is a peptide transition-state analogue that binds to the catalytic domain of human neutrophil collagenase; the complex's structure is deposited as 1MNC.⁴⁵ Different from the other complexes investigated, this protein employs a Zn atom (Zn 281) in ligand binding, which is nicely reproduced by the docking experiment (Figure 7). As in the case of decamethonium (4) binding to AChE, a full-MC run yields a ligand with the highest S_{Total} on the first rank, which is not structurally improved by further LMCS runs.

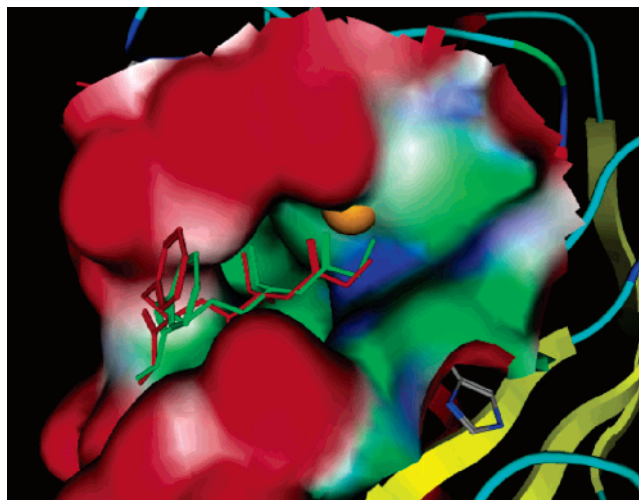


Figure 7. Overlay of methylamino-phenylalanyl-leucyl-hydroxamate (**8**) as predicted by QXP-MSD docking (red) on the X-ray structure (green). The ochre-colored ball denotes the Zn 281 atom bound to the hydroxamate structure of **8**.

Deoxythymidine (**9**), a substrate of the thymidine kinases (TK), and oxindole (ligand **10**), a known inhibitor of cyclin-dependent kinase 2, are two relatively rigid ligands tested with our QXP-MSD procedure. We have performed a series of unbound docking experiments with deoxythymidine (**7**), utilizing three different uncomplexed crystal structures of TK as templates, 1KI6, 1KI7, and 1KI8 (see Table 1).⁴⁵ The results are always compared to the original TK–deoxythymidine structure 1KIM.⁴⁵

The unbound docking of deoxythymidine (**9**) into 1KI6 yields an initial full-MC answer with the highest S_{Total} already on the first rank (RMSD of 0.43 Å). One additional LMCS run gives an energetically improved result with a slightly reduced RMSD of 0.74 Å. When 1KI7 is used as a protein template for docking deoxythymidine (**9**), three LMCS steps are necessary after the full-MC run to get the final answer with a RMSD of 1.11 Å. Finally, the docking of deoxythymidine into 1KI8 again gives the highest S_{Total} in the full-MC run already on the first rank. The structure is very similar to the final result, which is reached after one additional LMCS step.

Finally, the docking of oxindole (**10**), an inhibitor of cyclin-dependent kinase 2, was investigated in a bound docking experiment utilizing the corresponding protein 1FVT.⁴⁶ As shown in Table 9, QXP-MSD results in a final answer after a total of five QXP-MSD runs, in which the structure is energetically improved as compared to the initial solution from full-MC search conditions, although the full-MC search already resulted in a structure of the highest S_{Total} on the first rank with a very acceptable RMSD.

CONCLUSION

Molecular docking has become an important part of the drug development process. Docking procedures are very helpful in characterizing the protein–ligand interaction by providing predictions of the bound conformation for the ligand and a scheme for energetically ranking the protein–ligand interaction. Good structural predictions, however, depend on the correct scoring of docked poses, which is still regarded as one of the major challenges in the field of

Table 10. Comparison of Unbound Docking Results for BHG (**2**), E2020 (**3**), and Decamethonium (**4**) by Using QXP⁺,¹⁹ FlexX,¹⁶ and GOLD.^{21 a}

program	RMSD BHG (2)	RMSD E2020 (3)	RMSD decamethonium (4)	binding-site flexibility
QXP (MSD)	0.79	0.96	1.27	no
QXP (OSD)	2.35	2.19	1.27	no
QXP (SA)	1.71			yes

^a QXP was employed under standard conditions, which is one-step docking (OSD); MSD stands for multistep docking. RMSD (Å) was calculated using DAG53 (version 2) as a reference program.

molecular docking because dynamic and entropic factors are difficult to account for in docking procedures.

In this study, we described the development of a MSD procedure that allows for the correct pose prediction of ligands in its protein binding site, through a consensus scoring and ranking protocol, which is particularly useful in the treatment of highly flexible ligands. The procedure is based on the QXP program and makes use of the built-in local-MC algorithm in addition to the full-MC procedure. Rather than running a long docking process on a given conformation of a ligand, we use a limited number of cycles (though 10 000 in this investigation) to gain a new starting conformation for a subsequent docking run. A suitable starting conformation is derived from a consensus scoring of the 25 structures of a docking experiment. While only the initial docking run in the multistep process employs full-MC conditions for the pose prediction, all subsequent steps make use of the LMCS procedure with restricted rotational angles, by which the conformational search space is limited. The procedure reveals the importance of the starting conformation for a QXP-docking run. Only the S_{Total} scoring is capable of consistently finding an appropriate orientation and conformation of the ligand in the initial full-MC run, which then can be used for further refinement of the structure. This is demonstrated with the data of Table 6, which compares a multistep docking process on the basis of merely the E_{ass} data, the default ranking criterion of QXP. While the S_{Total} scoring usually gives a docking answer close to the best predictable solution already in the full-MC run, further LMCS steps only improve the structure in terms of energy with minor structural changes.

The method was developed particularly for highly flexible ligands, the structures of which often cannot be predicted correctly in a conventional docking experiment. Table 10 shows a comparison of results from docking BHG (**2**), E2020 (**3**), and decamethonium (**4**) into the AChE active site. While the standard procedure of QXP, one-step docking (OSD), does not give satisfying results for the first two structures, the MSD procedure for both exemplary ligands yields final structures with a RMSD < 1 Å compared to the crystal structure. As can be seen from Table 10, the MSD procedure is even preferred over simulated annealing conditions, using a protein binding site with flexible amino acid side chains. It should be noted, however, that the MSD procedure is computationally more expensive than the standard QXP technique. In addition, we have not yet automated the MSD procedure, and in some cases, we have to redefine the guide atoms for the definition of the cavity manually prior to the next run. Nevertheless, the examples shown in this investigation prove that the MSD procedure is necessary for a correct

docking or scoring answer. While, in some instances, QXP docking yields the correct answer with the highest S_{Total} already on the first rank (lowest E_{ass}), continuation of the docking procedure with a local Monte Carlo procedure (LMCS) turned out to be necessary in many other experiments in order to arrive at the correct structure (see, for example, the data for WIN52084 in Table 9).

We have demonstrated the QXP-MSD procedure to be a reliable tool with particular strength in the investigation of ligands with a high internal degree of freedom, which are the more difficult ones to predict. This was proven in bound and—more importantly—also in unbound docking studies. In this regard, two experiments are most notable: first, the correct unbound docking of the AChE inhibitor decamethonium that contains 11 rotatable single bonds and, second, the docking experiment with WIN51711 and WIN52084, which only differ in an additional methyl group in WIN52084 with respect to WIN51711, located at one end of the long stretched molecule of 20 carbon atoms ($\text{C}_{20}\text{H}_{28}\text{N}_2\text{O}_3$).

It should be mentioned that the RMSD algorithm in QXP, in some cases, gave a false positive answer, as demonstrated in Table 7. The saccharino ring of BHG (**2**) displays a pseudo- C_2 symmetry in which the carbonyl group and the sulfoxo group take opposite places in the structure. The docking of BHG (**2**) into 1QTI and 1EVE yields almost equally good RMSD values of 0.85 and 0.76 Å, respectively, despite the fact that the ligand in 1QTI has an inverted orientation. The literature provides other examples of how RMSDs can be misleading, as for instance shown in a recent publication by Kroemer et al.¹⁰ A visual inspection of docking results, therefore, is indispensable in evaluating docking answers. Though laborious, our new MSD procedure is highly suitable to yield correct pose predictions. Because of the relative simplicity of the method, it can be used directly in any docking calculation, thus providing a means to accurately score novel inhibitor candidates and to predict their bound conformation.

ACKNOWLEDGMENT

We thank Drs. D. Lamba, C. Bartolucci, and M. C. Siotto from the Institute of Crystallography, CNR, Trieste, Italy, for providing us with the crystal structure of BHG. We are also thankful to Dr. U. Jordis, Technical University of Vienna, who shared BHG data with us, particularly, the IC₅₀ value for AChE inhibition.

REFERENCES AND NOTES

- Muegge, I.; Rarey, M. Small Molecule Docking and Scoring. *Rev. Comput. Chem.* **2001**, *17*, 1–60.
- Kitchen, D. B.; Decornez, H.; Furr, J. R.; Bajorath, J. Docking and Scoring in Virtual Screening for Drug Discovery: Methods and Applications. *Nat. Rev. Drug Discovery* **2004**, *3*, 935–949.
- Mohan, V.; Gibbs, A. C.; Cummings, M. D.; Jaeger, E. P.; DesJarlais, R. L. Docking: Successes and Challenges. *Curr. Pharm. Des.* **2005**, *11*, 323–333.
- Congreve, M.; Murray, C. W.; Blundell, T. L. Structural Biology and Drug Discovery. *Drug Discovery Today* **2005**, *10*, 895–907.
- Wolfson, H. J.; Shatsky, M.; Schneidman-Duhovny, D.; Dror, O.; Shulman-Peleg, A.; Ma, B. Y.; Nussinov, R. From Structure to Function: Methods and Applications. *Curr. Protein Pept. Sci.* **2005**, *6*, 171–183.
- Abagyan, R.; Totrov, M. High-Throughput Docking for Lead Generation. *Curr. Opin. Chem. Biol.* **2001**, *4*, 375–382.
- Halperin, I.; Ma, B.; Wolfson, H.; Nussinov, R. Principles of Docking: An Overview of Search Algorithms and a Guide to Scoring Functions. *Proteins* **2002**, *47*, 409–443.
- Krovat, E. M.; Steindl, T.; Langer, T. Recent Advances in Docking and Scoring. *Curr. Comput.-Aided Drug Des.* **2005**, *1*, 93–102.
- Berman, H. M.; Westbrook, J.; Feng, Z.; Gilliland, G.; Bhat, T. N.; Weissig, H.; Shindyalov, I. N.; Bourne, P. E. The Protein Data Bank [http://www.rcsb.org/pdb/]. *Nucleic Acids Res.* **2000**, *28*, 235–242.
- Kroemer, R. T.; Vulpatti, A.; McDonald, J. J.; Rohrer, D. C.; Trosset, Y.; Giordanetto, F.; Cotesta, S.; McMartin, C.; Kihlen, M.; Stouten, P. F. W. Assessment of Docking Poses: Interactions-Based Accuracy Classification (IBAC) versus Crystal Structures Deviations. *J. Chem. Inf. Comput. Sci.* **2004**, *44*, 871–881.
- Davis, A. M.; Teague, S. J.; Kleywegt, G. J. Applications and Limitations of X-ray Crystallographic Data in Structure-Based Ligand and Drug Design. *Angew. Chem., Int. Ed.* **2003**, *42*, 2718–2736.
- Tame, J. R. H. Scoring Functions: A View from the Bench. *J. Comput.-Aided Mol. Des.* **1999**, *13*, 99–108.
- Toledo-Sherman, L. M. High-Throughput Virtual Screening for Drug Discovery in Parallel. *Curr. Opin. Drug Discovery Dev.* **2002**, *5*, 414–421.
- Waszkowycz, B. Structure-Based Approaches to Drug Design and Virtual Screening. *Curr. Opin. Drug Discovery Dev.* **2002**, *5*, 407–413.
- Schneidman-Duhovny, D.; Nussinov, R.; Wolfson, H. Predicting Molecular Interactions in Silico: II. Protein–Protein and Protein–Drug Docking. *J. Curr. Med. Chem.* **2004**, *11*, 91–107.
- Rarey, M.; Kramer, B.; Lengauer, T.; Klebe, G. A Fast Flexible Docking Method Using an Incremental Construction Algorithm. *J. Mol. Biol.* **1996**, *261*, 470–489.
- Ewing, T. J. A.; Kuntz, I. D. Critical Evaluation of Search Algorithms for Automated Molecular Docking and Database Screening. *J. Comput. Chem.* **1997**, *18*, 1176–1189.
- Welch, W.; Ruppert, J.; Jain, A. J. Hammerhead Fast, Fully Automated Docking for Flexible Ligands to Protein Binding Sites. *Chem. Biol.* **1996**, *3*, 449–462.
- McMartin, C.; Bohacek, R. S. J. Powerful, Rapid Computer Algorithms for Structure-Based Drug Design. *J. Comput.-Aided Mol. Des.* **1997**, *11*, 333–344.
- Morris, G. M.; Goodsell, D. S.; Halliday, R. S.; Huey, R.; Hart, W. E.; Belew, R. K.; Olson, A. J. Automated Docking Using a Lamarckian Genetic Algorithm and an Empirical Free Binding Energy Function. *J. Comput. Chem.* **1998**, *19*, 1639–1662.
- Jones, G.; Willet, P.; Glen, R. C.; Leach, A. R.; Taylor, R. Development and Validation of a Genetic Algorithm for Flexible Docking. *J. Mol. Biol.* **1997**, *267*, 727–748.
- Totrov, M.; Abagyan, R. Flexible Protein–Ligand Docking by Global Energy Optimization in Internal Coordinates. *Proteins* **1997**, *31*, 215–220.
- Axelsen, P. H.; Harel, M.; Silman, I.; Sussman, J. L. Structure and Dynamics of the Active Site Gorge of Acetylcholinesterase: Synergistic Use of Molecular Dynamics Simulation and X-ray Crystallography. *Protein Sci.* **1994**, *3*, 188–197.
- Taylor, P.; Radic, Z. The Cholinesterases: From Genes to Proteins. *Annu. Rev. Pharmacol. Toxicol.* **1994**, *34*, 281–320.
- Sussman, J. L.; Harel, M.; Frolova, F.; Oefner, C.; Goldman, A.; Tokar, L.; Silman, I. Atomic Structure of Acetylcholinesterase From Torpedo californica: A Prototypic Acetylcholine-Binding Protein. *Science* **1991**, *253*, 872–879.
- Pilger, C.; Bartolucci, C.; Lamba, D.; Tropsha, A.; Fels, G. Accurate Prediction of the Bound Conformation of Galanthamine in the Active Site of Torpedo Californica Acetylcholinesterase Using Molecular Docking. *J. Mol. Graphics Modell.* **2001**, *19*, 288–296.
- Linnemann, E.; Pilger, C.; Bartolucci, C.; Lamba, D.; Fels, G. Exploring the Inhibitor Binding-Site of Acetylcholinesterase. In *Proceedings of the 9th German–Japanese Workshop on Chem. Information*, May, 25–27, 2000; Science and Technology Agency of Japan, NRIM: Saitama, Japan, 2000; pp 87–90.
- Hardy, J.; Selkoe, D. J. The Amyloid Hypothesis of Alzheimer's Disease: Progress and Problems on the Road to Therapeutics. *Science* **2002**, *297*, 353–356.
- Feng, S.; Wang, Z. F.; He, X. C.; Zheng, S. X.; Xia, Y.; Jiang, H. L.; Tang, X. C.; Bai, D. L. Bis-huperzine B: Highly Potent and Selective Acetylcholine Sterase Inhibitors. *J. Med. Chem.* **2005**, *48*, 655–657.
- Greenblatt, H. M.; Guillou, C.; Guenard, D.; Argaman, A.; Botti, S.; Badet, B.; Thal, C.; Silman, I.; Sussman, J. L. The Complex of a Bivalent Derivative of Galanthamine with Torpedo Acetylcholinesterase Displays Drastic Deformation of the Active-Site Gorge: Implications for Structure-Based Drug Design. *J. Am. Chem. Soc.* **2004**, *126*, 15405–15411.
- Luttmann, E.; Linnemann, E.; Fels, G. Galanthamine as Bis-Functional Ligand for the Acetylcholinesterase. *J. Mol. Model.* **2002**, *8*, 208–216.
- Brooijmans, N.; Kuntz, I. D. Molecular Recognition and Docking Algorithms. *Annu. Rev. Biophys. Biomol. Struct.* **2003**, *32*, 335–373.

- (33) Trosset, J.-Y.; Scheraga, H. A. Reaching the Global Minimum in Docking Simulations: A Monte Carlo Energy Minimization Approach Using Bezier Splines. *Proc. Natl. Acad. Sci. U.S.A.* **1998**, *95*, 8011–8015.
- (34) Metropolis, N.; Rosenbluth, A. W.; Rosenbluth, M. N.; Teller, A. H.; Teller, E. Equation of State Calculations by Fast Computing Machines. *J. Chem. Phys.* **1953**, *21*, 1087–1092.
- (35) Mezei, M. Efficient Monte Carlo Sampling for Long Molecular Chains Using Local Moves, Tested on a Solvated Lipid Bilayer. *J. Chem. Phys.* **2003**, *118*, 3874–3879.
- (36) Jordis, U.; Froehlich, J.; Treu, M.; Hirschall, M.; Czollner, L.; Kaeltz, B.; Welzig, S. European Patent EP 1 181 294 B1.
- (37) Siotto, M.-C.; Bartolucci, C.; Lamba, D. The crystal structure will be published elsewhere. We thank the authors for providing us with the PDB file prior to publication.
- (38) Bartolucci, C.; Perola, E.; Pilger, C.; Fels, G.; Lamba, D. Three-Dimensional Structure of a Complex of Galanthamine (Nivalin) with Acetylcholinesterase from *Torpedo californica*: Implications for the Design of New Anti-Alzheimer Drugs. *Proteins* **2001**, *42*, 182–191.
- (39) Greenblatt, H. M.; Kryger, G.; Lewis, T.; Silman, I.; Sussman, J. L. Structure of Acetylcholinesterase Complexed with (–)-Galanthamine at 2.3 Å Resolution. *FEBS Lett.* **1999**, *463*, 321–326.
- (40) Kryger, G.; Silman, I.; Sussman, J. L. Structure of Acetylcholinesterase Complexed with E2020 (Aricept®): Implications for the Design of New Anti-Alzheimer Drugs. *Structure* **1999**, *7*, 297–307.
- (41) Harel, M.; Schalk, I.; Ehert-Sabatie, L.; Bouet, F.; Goeldner, M.; Hirth, C.; Axelsen, P. H.; Silman, I.; Sussman, J. L. Quaternary Ligand Binding to Aromatic Residues in the Active-Site Gorge of Acetylcholinesterase. *Proc. Natl. Acad. Sci. U.S.A.* **1993**, *90*, 9031–9035.
- (42) Hiremath, C. N.; Grant, R. A.; Filman, D. J.; Hogle, J. M. Binding of the Antiviral Drug win51711 to the Sabin Strain of Type-3 Poliovirus – Structural Comparison with Drug-Binding in Rhinovirus-14. *Acta Crystallogr., Sect. D* **1995**, *51*, 473–489.
- (43) Hadfield, A. T.; Oliveira, M. A.; Kim, K. H.; Minor, I.; Kremer, M. J.; Heinz, B. A.; Shepard, D.; Pevear, D. C.; Rueckert, R. R.; Rossman, M. G. Structural Studies on Human Rhinovirus 14 Drug Resistant Compensation Mutants. *J. Mol. Biol.* **1995**, *253*, 61–73.
- (44) Malkowski, M. G.; Ginell, S. L.; Smith, W. L.; Garavito, R. M. The Productive Conformation of Arachidonic Acid Bound to Prostaglandin Synthase. *Science* **2000**, *289*, 1933–1937.
- (45) Stams, T.; Spurlino, J. C.; Smith, D. L.; Wahl, R. C.; Ho, T. F.; Qoronfleh, M. W.; Banks, T. M.; Rubin, B. Structure of Human Neutrophil Collagenase Reveals Large S1' Specificity Pocket. *Nat. Struct. Biol.* **1994**, *1*, 119–123.
- (46) Champness, J. N.; Bennett, M. S.; Wien, F.; Visse, R.; Summers, W. C.; Herdewijn, P.; de Clercq, E.; Ostrowski, T.; Jarvest, R. L.; Sanderson, M. R. Exploring the Active Site of Herpes Simplex Virus Type-1 Thymidine Kinase by X-ray Crystallography of Complexes with Aciclovir and Other Ligands. *Proteins* **1998**, *32*, 350–361.
- (47) Davis, S. T.; Benson, B. G.; Bramson, H. N.; Chapman, D. E.; Dickerson, S. H.; Dold, K. M.; Eberwin, D. J.; Edelstein, M.; Frye, S. V.; Gampe, R. T.; Griffin, R. J.; Harris, P. A.; Hassell, A. M.; Holmes, W. D.; Hunter, R. N.; Knick, V. B.; Lackey, K.; Lavejoy, B.; Luzzio, M. J.; Murray, D.; Parker, P.; Rocque, W. J.; Shewchuk, L.; Veal, J. M.; Walker, D. H.; Kuyper, L. F. Prevention of Chemotherapy-Induced Alopecia in Rats by Cdk Inhibitors. *Science* **2001**, *291*, 134–137.
- (48) Go, N.; Scheraga, H. A. Calculation of the Conformation of cyclo-Hexaglycyl. 2. Application of a Monte-Carlo Method. *Macromolecules* **1978**, *11*, 552–559.
- (49) Greenblatt, H. M.; Dvir, H.; Silman, I.; Sussman, J. L. Acetylcholinesterase: A Multifaceted Target for Structure-Based Drug Design of Anticholinesterase Agents for the Treatment of Alzheimer's Disease. *J. Mol. Neurosci.* **2003**, *20*, 369–384.
- (50) Silman, I.; Sussman, J. L. Acetylcholinesterase: 'Classical' and 'Non-Classical' Functions and Pharmacology. *Curr. Opin. Pharmacol.* **2005**, *5*, 293–302.
- (51) Bourne, Y.; Taylor, P.; Radic, Z.; Marchot, P. Structural Insights into Ligand Interactions at the Acetylcholinesterase Peripheral Anionic Site. *EMBO J.* **2003**, *22*, 1–12.
- (52) Pang, Y. P.; Kozikowski, A. P. Prediction of the Binding Site of 1-Benzyl-4-[5,6-dimethoxy-1-indanon-2-yl)methyl]piperidine in Acetylcholinesterase by Docking Studies with the SYSDOC Program. *J. Comput.-Aided Mol. Des.* **1994**, *8*, 683–693.
- (53) Cormen, T. H.; Leiserson, C. E.; Rivest, R. L. *Introduction to Algorithms*; MIT Press: Cambridge, MA, 1990; Chapter 25.24.

CI050343M